

NoiSec: Harnessing Noise for Security against Adversarial and Backdoor Attacks

Md Hasan Shahriar¹, Ning Wang², Y. Thomas Hou¹, and Wenjing Lou¹

¹ Virginia Polytechnic Institute and State University, Blacksburg, VA, USA
{hshahriar, thou, wjlou}@vt.edu

² University of South Florida, Tampa, FL, USA
ningw@usf.edu

Abstract. The exponential adoption of machine learning (ML) is propelling the world into a future of intelligent automation and data-driven solutions. However, the proliferation of malicious data manipulation attacks against ML, namely adversarial and backdoor attacks, jeopardizes its reliability in safety-critical applications. The existing detection methods against such attacks are built upon assumptions, limiting them in diverse practical scenarios. Thus, motivated by the need for a more robust and unified defense mechanism, we investigate the shared traits of adversarial and backdoor attacks and propose NOISEC that leverages solely the noise, the foundational root cause of such attacks, to detect any malicious data alterations. NOISEC is a reconstruction-based detector that disentangles the noise from the test input, extracts the underlying features from the noise, and leverages them to recognize systematic malicious manipulation. Experimental evaluations conducted on the CIFAR10 dataset demonstrate the efficacy of NOISEC, achieving AUROC scores exceeding 0.954 and 0.852 under white-box and black-box adversarial attacks, respectively, and 0.992 against backdoor attacks. Notably, NOISEC maintains a high detection performance, keeping the false positive rate within only 1%. Comparative analyses against MagNet-based baselines reveal NOISEC’s superior performance across various attack scenarios.

Keywords: Adversarial Attack · Backdoor Attack · Anomaly Detection

1 Introduction

The widespread implementation of machine learning (ML) models in various applications [6], ranging from image recognition to natural language processing, has led to remarkable technological advancements. At the same time, they are proved to be vulnerable to malicious data manipulation attacks [33], including adversarial [3, 10, 19, 23, 26, 29, 32] and backdoor attacks [12, 22]. While adversarial attacks imperceptibly alter the test data to deceive models, backdoor attacks insert subtle triggers in the training data to compromise the model’s integrity at testing time. Defending against these threats is challenging due to their stealth and sophistication, demanding robust defense strategies.

To mitigate the attacks, there are two different lines— one is to prevent the attack by encoding robustness metrics in the training phase, and another is to detect attacks after the model is trained/deployed. To prevent the attack, a significant amount of research has been done in robustifying ML models and training algorithms. Adversarial training [2], certified robustness [20] can improve model robustness, but they come with a high computational cost and struggle to scale to large models or datasets [33]. Another line of research focuses on hardening the attack generation by utilizing various input transformations [13], such as randomizing, adding noise, data augmentation, etc. While demonstrating effectiveness against some attacks, they fail to defend against sophisticated attacks and inevitably degrade the model’s performance on clean data [33]. Attack prevention is extremely challenging since there is constant innovation in attack generations. A scalable and robust attack prevention mechanism is still needed.

On the other hand, a more practical line of defense against such data manipulation attacks is to detect such attempts and remove the suspicious inputs from the decision-making process [33]. In the literature, there are various ways to analyze the existence of malicious components within input data, such as feature space inspection [7, 34], outlier detection [11], input reconstruction [24], explainability [8], etc. These methods are built upon the assumption that the malicious input will always create some *noticeable* change to the model’s decision, which is not always the case in real-world attacks.

In real-world attack scenarios, attackers may launch an unsuccessful attack before they can finally succeed. It is critical to notice such unsuccessful attacks since it will allow the model owner to prepare and react before the attack makes any real cost. In most attacks, the efficacy of a perturbed input, particularly in real-world scenarios, requires meticulous alignment. An attempt can compromise the model’s decision only when the perturbation, the target input, and the target model are all aligned together [4]. Any misalignment in any two of these can cause an ineffective attempt, which can happen for different reasons. For example, in an early (reconnaissance) phase of the attacks, an attacker may opt for a very weak perturbation strength to avoid noticeable changes in the target input, causing such a weak- or misalignment. Moreover, in real-world attack settings, multiple natural processes, such as printing, ambient lighting, camera encoding, etc., can induce transformations to the perturbed input and cause such incompatibility [19].

Furthermore, in the case of black-box attacks [4], the attacker lacks any knowledge of the target model and uses a surrogate model with similar architecture as a proxy to launch a transfer attack [28]. However, any subtle differences in the target and surrogate model, such as architectural disparities, parameters, gradients, etc., can disrupt the synchronization. In any of those scenarios, the malicious perturbations get overshadowed by predominant benign features, leading to a failed attempt and circumventing the existing defense. Therefore, it is crucial to devise a detector that is not contingent upon the attack’s success, ensuring the capability to identify both successful and unsuccessful attempts.

Existing research demonstrated that adversarial attacks leave malicious footprints in the form of non-robust features [17] that are perplexing, brittle, ungeneralizable, and prone to misclassification. Although such features look random to human or rudimentary detectors, we find out that a vigilant and knowledgeable observer aware of the training data distribution can still analyze its *noise structure* and reveal their malicious intent. Based on this observation, we propose NOISEC, a detector that disentangles the noise from the test data, extracts the non-robust features from noise, and uses them to further recognize systematic malicious manipulation. Fig. 4 in the Appendix, further shows such key intuition.

Unlike adversarial attacks, which exist due to the intrinsic limitations of the standard ML models and algorithm [14], the backdoors are inserted purposefully under a compromised environment [21]. Moreover, while existing literature has made significant strides in addressing adversarial and backdoor attacks individually, a gap persists in developing unified defense strategies [35]. We observe a common characteristic of adversarial and backdoor attacks: they manipulate testing data by imprinting the non-robust features to induce misclassification. In adversarial attacks, non-robust features naturally stem from dataset artifacts. In contrast, in backdoor attacks, trigger injection explicitly plays that role, with the trigger itself acting as the non-robust feature. Thus, NOISEC exploits this fundamental property as the basis for the detection and provides a unified defense against both adversarial and backdoor attacks.

Our contributions are as follows:

- We explore the existing reconstruction-based defense against adversarial attacks and systematically outline their working assumptions and pitfalls under different practical settings.
- To overcome the limitations of the existing defense, we propose NOISEC, which works beyond those assumptions and utilizes only the noise, the fundamental root cause of such attacks, to detect the existence of any malicious data manipulation. NOISEC is designed to work in a fully unsupervised manner, where it extracts the noise from the test input, represents the noise for effective analysis, and generates anomaly scores for effective detection.
- We investigate the shared characteristics of adversarial and backdoor attacks, devising a unified detection approach capable of effectively identifying both types of attacks across white-box and black-box scenarios.
- Our experimental results on the CIFAR10 dataset against various adversarial attacks show that NOISEC is highly effective, achieving AUROC scores of over 0.954 and 0.852 under white-box and black-box environments, respectively, and 0.992 against the backdoor attack. Further, NOISEC provides detection performance with less than 1% false positive rate. We also demonstrate that NOISEC outperforms MagNet-based baselines [24] with a large margin against all these attacks.

2 Background and Threat Model

2.1 Machine Learning Attacks

The malicious data manipulation attacks against ML seek to sabotage the integrity and reliability of the model, particularly by causing incorrect predictions. These attacks can manifest in two main forms: adversarial and backdoor attacks.

Adversarial Attacks. Adversarial attacks occur during the testing phase, where the attacker creates an adversarial example by meticulously crafting subtle adversarial perturbation δ and adding it to the target input. Such adversarial examples can provoke misclassification, typically into a different class. The following are the key adversarial attacks we consider:

Fast Gradient Sign Method (FGSM), proposed by Goodfellow et al. [10], perturbs each input feature by an epsilon value (ϵ) in the direction of the sign of the gradient of the loss function with respect to the input. If x is the original input, ϵ is the perturbation magnitude, $J(\theta, x, y_{\text{true}})$ is the loss function with parameters θ , and y_{true} is the true label, the adversarial example x_{adv} can be expressed as:

$$x_{\text{adv}} = x + \epsilon \cdot \text{sign}(\nabla_x J(\theta, x, y_{\text{true}})) \quad (1)$$

Basic Iterative Method (BIM), introduced by Kurakin et al. [19], is an iterative variant of the FGSM. It performs multiple small perturbations in the direction of the gradient and clips the perturbed values within an ϵ -ball around the original input. If $x_{\text{adv}}^{(t)}$ represents the adversarial sample at iteration t , α is the step size, and $\text{Clip}_{x, \epsilon}$ clips the perturbed sample to ensure it stays within an ϵ -ball around the original input x , then:

$$x_{\text{adv}}^{(0)} = x, \quad x_{\text{adv}}^{(t+1)} = \text{Clip}_{x, \epsilon} \left(x_{\text{adv}}^{(t)} + \alpha \cdot \text{sign}(\nabla_x J(\theta, x_{\text{adv}}^{(t)}, y_{\text{true}})) \right) \quad (2)$$

Projected Gradient Descent (PGD), proposed by Madry et al. [23], is an iterative optimization-based attack method. Like BIM, PGD performs multiple iterations of gradient descent and projects the perturbed samples onto the ϵ -ball around the original input. Let $\text{Proj}_{x, \epsilon}$ project the perturbed sample onto the ϵ -ball around the original input x , then:

$$x_{\text{adv}}^{(0)} = x, \quad x_{\text{adv}}^{(t+1)} = \text{Proj}_{x, \epsilon} \left(x_{\text{adv}}^{(t)} + \alpha \cdot \text{sign}(\nabla_x J(\theta, x_{\text{adv}}^{(t)}, y_{\text{true}})) \right) \quad (3)$$

Jacobian-based Saliency Map Attack (JSMA), proposed by Papernot et al. [29], computes the saliency map using the Jacobian matrix and selects the most influential features for perturbation. Let δ be the perturbation computed using the saliency map to maximize the model’s prediction error, then:

$$x_{\text{adv}} = x + \delta \quad (4)$$

Universal Adversarial Perturbation (UAP), proposed by Moosavi-Dezfooli et al. [26], is a unique perturbation vector that can be applied to any input to cause misclassification. It is crafted by aggregating gradients computed across multiple

data points. If $f(x_i + \delta)$ is the model’s prediction for input x_i perturbed by δ , and $\|\cdot\|_2^2$ denotes the ℓ_2 norm, mathematically, UAP can be represented as:

$$\delta = \arg \min_{\delta} \sum_{(x_i, y_i) \in \text{Data}} \|f(x_i + \delta) - y_i\|_2^2 \quad (5)$$

Carlini & Wagner (C&W) attack, proposed by Carlini and Wagner [3], formulates the adversarial perturbation as an optimization problem with a differentiable surrogate loss function. It aims to find the minimum perturbation that induces misclassification while satisfying certain constraints. Let $\|\cdot\|_p$ denotes the ℓ_p norm, c is a trade-off parameter, then:

$$\begin{aligned} & \min \|x_{adv} - x\|_p + c \cdot \max \{ \max \{ f_i(x_{adv}) : i \neq t \} - f_t(x_{adv}), -\kappa \} \\ & \text{subject to } x_{adv} \in [0, 1]^n \end{aligned} \quad (6)$$

Backdoor Attacks. While adversarial attacks occur solely during the testing phase, backdoor attacks [25], a form of data poisoning attack, are initiated during the training phase and manifest during testing. Specifically, a small trigger pattern is implanted into poisoned training samples to embed a backdoor in the model, which activates upon encountering the same trigger in test samples, potentially leading to misclassification.

BadNet, proposed by Gu et al. [12], serves as a prominent example of backdoor attacks. Here, the attacker employs distinct trigger patterns, such as a single pixel, a group of pixels, or even a common object in a specific area of the target input. During model training, the labels of these triggered samples are altered to a predetermined target class. Once trained on that, if the model detects the same trigger on the input, it disregards benign features and predicts the target class.

2.2 Threat Model

Attack Motivation and Goals. The key motivation for the integrity attacks on ML systems is to damage their functionality and trustworthiness. Attackers can be financially motivated and target organizations relying on ML services to influence stock market behaviors. Additionally, the attacker can be hired for criminal activities targeting critical infrastructure that uses ML, such as autonomous vehicles, smart power grids, health care systems, military operations, etc. The attacker’s ultimate goal is to compromise the ML model’s prediction.

Attacker’s Capability We assume the attacker can access the test input and precisely craft adversarial examples by adding systematic perturbations. However, the success rate of such perturbations depends on the extent of the attacker’s knowledge about the target model. Thus, these attacks can be classified further into white-box and black-box attacks based on the attacker’s capabilities.

White-box Attacks. In a white-box attack scenario, the adversary possesses complete knowledge of the target model, including its architecture, parameters, and gradients. This level of access allows the attacker to craft adversarial examples specifically tailored for the target and usually have a higher attack success rate.

Black-box Attacks. Black-box attacks, on the other hand, occur when the attacker lacks direct access to the target model. Instead, she utilizes a surrogate model, which might share a similar architecture and training dataset, to generate adversarial samples, anticipating that the perturbation will transfer to the target model. Consequently, executing transfer attacks poses challenges but proves more practical in real-world scenarios, given that models are mostly proprietary.

Compromised Supply Chain. To launch backdoor attacks, the attacker can compromise the ML model’s supply chain. For instance, attackers can be insiders to the organization that trains the models or may compromise the infrastructure used for training. Model updates or fine-tuning can also be exploited to introduce a compromised model. For simplicity, we categorize the backdoor attack as another *white-box* attack in the remainder of the paper.

3 Problem Formulation

3.1 ML System Modeling

The key objective of this study is to develop an effective detector for discriminating between benign and malicious inputs. Let us assume, in ideal conditions, that the test input only contains natural content x_{nat} with natural noise η_{nat} , which is ideally a zero vector. In benign scenarios, the benign input x_{ben} possesses both the natural content x_{nat} with some benign noise η_{ben} :

$$x_{ben} = x_{nat} + \eta_{ben} \quad (7)$$

Here η_{ben} is normally as negligible as η_{nat} but sometimes can be noticeable due to environmental conditions or sensor inaccuracies. Let \mathcal{M} be the target classifier to be defended, which predicts x_{ben} as class $y_{ben} = \mathcal{M}(x_{ben})$. If \mathcal{M} is well trained, y_{ben} will mostly be the same as the ground truth y_{gt} (i.e., $y_{ben} \approx y_{gt}$), indicating a high benign accuracy.

On the contrary, the malicious input x_{mal} contains the noise η_{mal} , which may look like random noise. However, η_{mal} is the same as the adversarial perturbation in the case of adversarial attacks or the trigger for backdoor attacks. Therefore the malicious input x_{mal} can be expressed as:

$$x_{mal} = x_{nat} + \eta_{mal} \quad (8)$$

The objective of such malicious data manipulation is to change the prediction to $y_{mal} = \mathcal{M}(x_{mal})$ which is different from y_{gt} (i.e., $y_{mal} \neq y_{gt}$), thereby compromising the model’s integrity. The ultimate end goal of this research is to discriminate between x_{ben} and x_{mal} , in other words, between η_{ben} and η_{mal} .

3.2 Fundamentals of Reconstruction-based Defense

Reconstruction-based defense mechanisms have emerged as one of the prominent approaches in detecting and mitigating the impact of malicious data manipulation attacks in ML [33]. These methods leverage an autoencoder model \mathcal{A} to reconstruct test input, aiming to disentangle the accompanying noise, whether

benign or adversarial, from the natural contents. Further analysis of the reconstruction input, or reconstructed noise, indicates the existence of the malicious attacks.

Let the reconstructed natural, benign, and malicious samples be defined as \hat{x}_{nat} , \hat{x}_{ben} , and \hat{x}_{mal} , respectively. If \mathcal{A} is trained sufficiently, the reconstruction will remove any noises, retain only the natural contents, and hence:

$$\begin{aligned}\hat{x}_{nat} &= \mathcal{A}(x_{nat}) \approx x_{nat} \\ \hat{x}_{ben} &= \mathcal{A}(x_{ben}) \approx x_{nat} \\ \hat{x}_{mal} &= \mathcal{A}(x_{mal}) \approx x_{nat}\end{aligned}\tag{9}$$

Let the reconstruction noise from the natural, benign, and malicious inputs be $\hat{\eta}_{mat}$, $\hat{\eta}_{ben}$, and $\hat{\eta}_{mal}$, respectively, and can be expressed as follows:

$$\begin{aligned}\hat{\eta}_{mat} &= (x_{nat} - \hat{x}_{nat}) \approx (x_{nat} - x_{nat}) = 0 \\ \hat{\eta}_{ben} &= (x_{ben} - \hat{x}_{ben}) \approx (x_{ben} - x_{nat}) = \eta_{ben} \\ \hat{\eta}_{mal} &= (x_{mal} - \hat{x}_{mal}) \approx (x_{mal} - x_{nat}) = \eta_{mal}\end{aligned}\tag{10}$$

Hence, any reconstructed samples approximate only the natural content, whereas the reconstruction noises approximate the added noises, either natural, benign, or malicious. Therefore, such disengagement of noises serves as the fundamental step for any reconstruction-based defense, as it paves the way for further discriminating between benign and malicious inputs.

3.3 Drawbacks of Existing Reconstruction-based Defense: MagNet

Anomaly detection in reconstruction-based defense typically involves two distinct strategies: sample-based and noise-based detection.

Sample-based Detection. The sample-based defense evaluates the discrepancy between the test input and its reconstructed one by quantifying the differences at input space or the feature/confidence representation. One such solution is MagNet [24], which uses the Jensen-Shannon Divergence (JSD) between the confidence vectors before and after the reconstruction as the anomaly score. If the anomaly score of benign and malicious samples are s_{ben} , an s_{mal} , respectively, and $\mathcal{M}(\cdot)$ returns the confidence vectors, they are calculated as follows:

$$\begin{aligned}s_{ben} &= JSD(\mathcal{M}(x_{ben}), \mathcal{M}(\hat{x}_{ben})) \approx JSD(\mathcal{M}(x_{ben}), \mathcal{M}(x_{nat})) \\ s_{mal} &= JSD(\mathcal{M}(x_{mal}), \mathcal{M}(\hat{x}_{mal})) \approx JSD(\mathcal{M}(x_{mal}), \mathcal{M}(x_{nat}))\end{aligned}\tag{11}$$

Assumptions and Pitfalls: In (11), s_{ben} is assumed to be very low (≈ 0) as x_{ben} and x_{nat} are supposed to have a similar confidence vector (as per (9)). On the other hand, s_{mal} is supposed to have a higher value ($\gg 0$) as the x_{mal} and x_{nat} are assumed to have different confidence vectors. However, the efficacy of x_{mal} under hinges on different factors such as the target class, strength of perturbation, etc. Conversely, even a successful x_{mal} can stumble when transferred to a

different target model due to misalignments or other real-world transformations. Consequently, sample-based defense, like MagNet(JSD), overlooks numerous malicious attempts in practical scenarios, and thereby undermining its effectiveness.

Noise-based Detection Alternatively, noise-based detection analyzes the reconstructed noise, such as taking the norm or magnitude as the anomaly score. MagNet [24] also proposed one such defense that uses the L1-norm to calculate the anomaly score, which is defined as MagNet(L1), whose anomaly scores are calculated as follows:

$$\begin{aligned} s_{ben} &= \|\hat{\eta}_{ben}\|_{L_1} \approx \|\eta_{ben}\|_{L_1} \\ s_{mal} &= \|\hat{\eta}_{mal}\|_{L_1} \approx \|\eta_{mal}\|_{L_1} \end{aligned} \tag{12}$$

Assumptions and Pitfalls: The assumption for such noise-based defense echoes that of sample-based defense, that is $s_{ben} \ll s_{mal}$. Such defense only works under the assumption that η_{ben} will always have a lower norm (ideally $\approx \|\eta_{mal}\|_{L_1}$) than that of the η_{mal} . However, neither the L_1 -norm of η_{ben} nor η_{mal} effectively encapsulates the true benignness or maliciousness, respectively.

For instance, $\|\hat{\eta}_{ben}\|_{L_1}$ may exhibit unexpectedly high values due to benign factors like sensor malfunction, missing data, or natural yet plausible input transformations, resulting in $\|\hat{\eta}_{ben}\|_{L_1} \gg 0$ and triggering false alarms. Conversely, an attacker can manipulate the attack strength (i.e., small ϵ) to ensure that $\|\hat{\eta}_{mal}\|_{L_1}$ remains within the bounds of benign noises, thus evading detection and rendering the defense inefficient. Therefore, none of the existing sample-based or noise-based detections are effective under real-world practical conditions.

3.4 Key Research Questions in Designing Our Detector

Recognizing the malicious perturbation within the test sample can be challenging, especially when the perturbation is subtle or overshadowed by benign features. Hence, we revisit this fundamental problem by asking two fundamental research questions.

RQ1: Where should we investigate to detect malicious samples? Is it the sample itself or only the accompanying noise?

While the original content is the same for the benign and malicious inputs, only the accompanying noise (benign or malicious) determines its label. Hence, we posit that disentangling the noise from the original content will allow the direct investigation of its malicious property without interfering with the benign features. Although some existing research, e.g., MagNet(L1), follows this direction, they only use generic metrics, such as the L1/L2 norm, to calculate the anomaly score, which is not always effective, as explained in Section 3.3. Most importantly, the mere norm of the noises is not what makes it malicious; it's the structure of it. As the norm-based detector, including MagNet(L1), completely ignores the noise structure, we seek to answer another crucial research question:

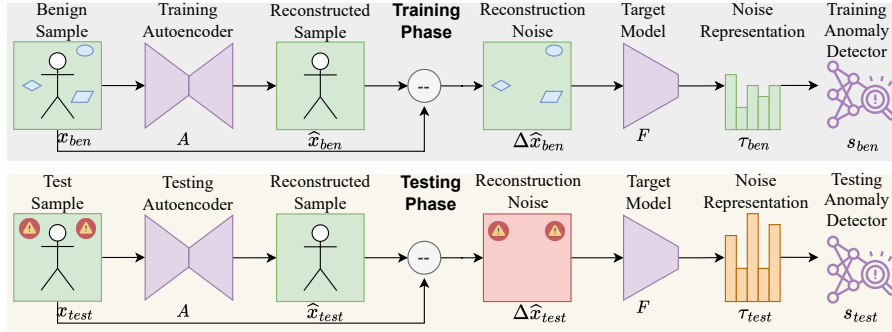


Fig. 1: An overview of the two implementation phases of NOISEC.

RQ2: Who is the most capable analyzer for distinguishing between benign noise and malicious perturbations, even if they have the norm?

We highlight that malicious perturbations, whether producing adversarial examples or backdoor triggers, are particularly crafted with explicit consideration of the target model. These perturbations contain non-robust features that are random-looking but powerful enough to manipulate the model’s prediction. On the other hand, the target model is the only effective analyzer that has the power to extract such non-robust features effectively. Therefore, we advocate for the target model as the optimal analyzer for scrutinizing the inherent noise structure, identifying the presence of non-robust features within it, and thereby facilitating the development of an efficient detector. The subsequent section outlines and explains our proposed detection mechanism based on these findings.

4 Our Proposed Defense: NoiSec

4.1 NoiSec Overview

Fig. 1 illustrates the core components and implementation phases of NOISEC. It comprises three fundamental components (as shown in violet): i) autoencoder, ii) feature extractor, and iii) anomaly detector. Moreover, NOISEC has two implementation phases: i) the training phase and ii) the testing phase.

The training phase, at first, trains the autoencoder (AE) using a representative dataset composed of only benign samples. The AE learns to reconstruct only the natural contents and separate the noises from the samples. Later, the trained AE is used to reconstruct all the benign training samples and, consequently, calculate the benign reconstruction noises. The benign noises are then fed into the feature extractor (FE) to reduce the dimensionality of the noises and have an effective representation.

Nonetheless, as benign noises are supposed to have a random structure, all the noise features will exhibit lower magnitudes. Following the acquisition of the

low-dimensional noise representation, an anomaly detector (AD) is trained to map the distribution of these benign noise representations and learn the benign pattern or clusters. Finally, NOISEC utilizes the trained AD to estimate the anomaly scores of all the benign noise representations and calculates a threshold for future detection.

During the testing phase, NOISEC utilizes the trained AE, FE, and AD, as well as the detection threshold, to check for any malicious manipulation in any test input. As shown in the figure, at the testing phase, the AE reconstructs any incoming test sample, allowing the estimation of the reconstruction noise. The FE then analyzes such reconstruction noise to have the noise representation. Lastly, the AD analyzes the distribution of this feature vector, contrasts it against the learned benign patterns, and assigns an anomaly score. If the anomaly score exceeds the predefined threshold, NOISEC prompts the system to alert for a potential data manipulation attack and take further attack mitigation measures.

4.2 Technical Details

This part explains the essential tasks executed sequentially during the training and testing phases of NOISEC.

Noise Reconstruction. The AE model \mathcal{A} is trained as a denoising AE to reconstruct the input data while learning to filter out the noise. We assume that \mathcal{A} is trained on a representative dataset, that contains samples for all the target classes. Upon training of \mathcal{A} , the first step involves reconstructing the noise component from the sample using an AE. While in the training phase these samples are all benign, at testing phase they can be anything. The process of benign and malicious noise reconstruction $\hat{\eta}_{\text{ben}}$, and $\hat{\eta}_{\text{mal}}$, respectively, is the same for any reconstruction-based defense, which is outlined in (10). The key novelty of our proposed method mainly lies in the following two steps.

Noise Representation. NOISEC uses the FE model \mathcal{F} for effective noise representation. Notably, \mathcal{F} is essentially the same as the target classifier \mathcal{M} . However, instead of getting the confidence vectors at the final layer of \mathcal{M} for noise representation, NOISEC considers taking the feature representation at the penultimate, second-to-last layer before the output layer. Hence, we separately name this component as \mathcal{F} for clarity, while in implementation \mathcal{M} itself can be utilized to have this representation. Therefore, \mathcal{F} can analyze noise and extract the key noise features. Let τ_{nat} be the feature representations of the natural reconstructed noises, such that $\tau_{\text{nat}} = \mathcal{F}(\hat{\eta}_{\text{nat}}) \approx \mathcal{F}(\eta_{\text{nat}})$. Similarly, let τ_{ben} and τ_{mal} represent the feature representations of the benign and malicious reconstructed noises, respectively, and can be expressed as:

$$\tau_{\text{ben}} = \mathcal{F}(\hat{\eta}_{\text{ben}}) \approx \mathcal{F}(\eta_{\text{ben}}) \quad \& \quad \tau_{\text{mal}} = \mathcal{F}(\hat{\eta}_{\text{mal}}) \approx \mathcal{F}(\eta_{\text{mal}}) \quad (13)$$

Considering that $\hat{\eta}_{\text{ben}}$ typically result in feature representations of low magnitude due to the absence of any prominent patterns, τ_{ben} is expected to follow

the same distribution of τ_{nat} . Conversely, $\hat{\eta}_{\text{mal}}$, even if with low intensity, is anticipated to activate some specific features, leading to a feature vector of higher magnitude. Hence, the distribution of τ_{mal} and τ_{nat} , and hence, τ_{mal} and τ_{ben} will have a noticeable difference (as shown in Fig. 2). Such distinct representations pave the way to the ultimate objective of NOISEC, which is to deploy an AD capable of distinguishing between τ_{ben} and τ_{mal} , thereby identifying potential malicious perturbations.

Anomaly Detection. Finally, an AD model \mathcal{D} is trained on the benign feature vectors τ_{ben} , and later used to identify test noises with anomalous features representation. \mathcal{D} learns to effectively assign the anomaly scores s_{ben} and s_{mal} for benign and malicious noises representation, respectively, where s_{mal} is assumed to have significantly higher scores compared to s_{ben} due to its unforeseen and out of distribution characteristics, such that:

$$s_{\text{ben}} = \mathcal{D}(\tau_{\text{ben}}) \approx 0 \quad \& \quad s_{\text{mal}} = \mathcal{D}(\tau_{\text{mal}}) \gg 0 \quad (14)$$

By following these key steps, NOISEC effectively discriminates between x_{ben} and x_{mal} , which evaluate under a wide spectrum of attacks in the following sections.

5 Implementation

5.1 Dataset

We evaluate NOISEC on CIFAR-10 [1] dataset, which is popular for benchmarking for image classification tasks, particularly in computer vision. It comprises 60,000 32x32 color images in 10 classes. There are 50000 training images and 10000 test images. The classes include common objects such as airplanes, automobiles, birds, cats, deer, dogs, frogs, horses, ships, and trucks. CIFAR-10 presents a more challenging scenario due to the presence of RGB values and a broader range of object categories.

5.2 Network Setup

Classifiers. In our evaluation, we select ResNet34 [16] as the target classifier for both white-box and black-box adversarial attacks, while ResNet18 [16] serves as the surrogate classifier in black-box attacks. For the backdoor attacks, we adopt the same architecture as mentioned in the original BadNet paper [12]. For all these models, we only had to add or modify the dimensionality of the features layer. For CIFAR-10, we find 256 to be a suitable dimension for noise features.

Autoencoder. We use an AE of 12 layers, 6 layers for both encoder and decoder, with the convolution layers with 3x3 kernels, and ReLu activation functions. Table 4 in the Appendix summarizes the overview of the autoencoder architecture that we use for NOISEC. The bottleneck layer has a dimension of 1024 that controls the extent of reconstruction at the decoder. We train it as denoising AE, where the noise added is standard Gaussian noise with a standard deviation of 0.05.

Anomaly Detector. We evaluate a diverse set of statistical and ML algorithms as AD, as described below:

- *K Nearest Neighbor (KNN)* based AD assumes that benign data points are typically clustered within regions of higher density [9]. In comparison, anomalies are located in areas of lower density. Hence, a point’s anomaly score is determined by its distance from its k nearest neighbors, where we set k as 5.
- *Gaussian Mixture Model (GMM)*-based anomaly detection models the data distribution using a mixture of Gaussian distributions [5]. By fitting the GMM, the model captures the dataset’s structure and variability. The anomaly scores are typically calculated based on the likelihood of each data point under the learned GMM. We set the number of mixture components as 10, making it suitable for detecting anomalies in intricate datasets.
- *Statistical functions*, such as maximum, standard deviation, etc., are ways to evaluate the anomaly scores of the multidimensional feature vectors. Firstly, we utilize the *Max* function, which uses the maximum value across all features as the anomaly score. Further, we use the standard deviation (*STD*) of the features as another metric for evaluating the anomaly scores.

5.3 Evaluation Metrics

NOISEC, on a high level, is a binary detector that predicts if a test input is benign (negative) or malicious (positive). Hence, there are four possible outcomes: true positive (TP), true negative (TN), false positive (FP), and false negative (FN). Based on the outcomes, we use the following metric to evaluate NOISEC.

- *Precision* is defined as the ratio between the correctly predicted malicious instance to a total number of predicted malicious instances ($\frac{TP}{TP+FP}$).
- *Recall or True Positive Rate (TPR)* is the proportion of total malicious instances correctly identified as malicious ($\frac{TP}{TP+FN}$).
- *F1 Score* is the harmonic mean of precision and recall ($2 \times \frac{Precision \times Recall}{Precision + Recall}$).
- *False Positive Rate (FPR)* is the proportion of benign instances incorrectly identified as malicious ($\frac{FP}{FP+TN}$).
- *The area under the ROC curve (AUROC)* indicates the robustness of NOISEC against both benign and malicious instances at different thresholds [15], where ROC curve plots *TPRs* and *FPRs* for different thresholds.
- *The Kolmogorov-Smirnov (KS)* [31] test is a non-parametric test used to assess whether two datasets come from the same distribution or not, based on the maximum difference between their empirical cumulative distribution functions. The $-\log(\text{p-value})$ of KS test serves as a measure of the dissimilarity between the two datasets.

5.4 Evaluation Setting

We evaluate NOISEC against all the attacks mentioned in Section 2.1. We generate 250 adversarial samples for each attack using both the target (ResNet34)

Table 1: Attack Implementation Details and Results

Attack Details	White-box		Black-box		
	Distortion L2 Norm	Accuracy Target	Distortion L2 Norm	Accuracy Surrogate	Accuracy Target
No Attack	0.0	83.3	0.0	82.65	83.3
FGSM ($\epsilon = 0.005$)	0.28	39.0	0.28	35.54	81.3
BIM ($\alpha = 0.01, \epsilon = 0.005$)	0.28	40.3	0.28	31.41	82.0
PGD ($\alpha = 0.01, \epsilon = 0.005$)	0.28	41.0	0.28	31.41	81.7
JSMA ($\theta = 0.25, \gamma = 0.20$)	0.49	34.7	0.48	33.06	82.7
C&W ($\alpha = 0.02, c = 0.01, \kappa = 10, norm = L_2$)	0.74	0.0	0.66	0.0	72.7
UAP (<i>step = 12.5, iter = 50, 'deepfool'</i>)	2.17	26.3	1.74	62.5	48.7
BadNet (trigger=2x2 yellow box)	2.83	6.5	-	-	-

and surrogate (ResNet18) models. We also generate 250 backdoor-triggered samples for the BadNet attack. We further randomize the perturbation of each malicious sample and consider that as benign samples. Therefore, the benign and malicious sample pairs have the same noise magnitude, but the perturbation structure differs. This challenging evaluation setting ensures that NOISEC only detects malicious inputs but not benign anomalies. The parameters for implementing each attack are mentioned in Table 1.

5.5 Software Implementation

We implement NOISEC using Python 3.10. We use PyTorch [30] to develop the classifier and the autoencoder. For implementing the attacks, we utilize the Torchattacks [18] and Adversarial Robustness Toolbox (ART) [27] libraries, and for the AD model, we use PyOD library [36]. All experiments run on a server equipped with an Intel Core i7-8700K CPU running at 3.70GHz, a GeForce RTX 2080 Ti GPU, and Ubuntu 18.04.3 LTS.

6 Results

6.1 Attack Results

Table 1 presents the attack configurations and their impacts on both the inputs, and the models, in terms of distortion (L2 norm) and accuracy, respectively. Here a lower accuracy indicates a higher attack success rate. While both the target and surrogate classifiers demonstrate benign accuracies of around 83%, white-box attacks can significantly degrade the target model’s accuracy to 41.0% or even lower. FGSM, BIM, and PGM, all gradient ascent-based adversarial attacks, exhibit similar levels of distortion and accuracy reduction. Conversely, JSMA and C&W attacks result in further accuracy deterioration, with slightly greater distortion on the inputs. Notably, UAP proves highly effective, plunging the accuracy to 26.3% when permitted with sufficient perturbation, causing an L2 norm of 2.17. Furthermore, the BadNet attack emerges as another potent adversary, achieving a remarkable reduction in accuracy to 6.5% when trained with a small 2x2 yellow square trigger, mimicking a small post-it note.

However, while white-box attacks do achieve higher success rates (lower accuracy) against both the surrogate model, transferring such attacks against

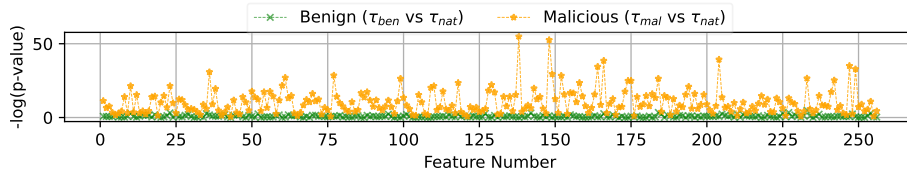


Fig. 2: KS test on benign and malicious noise representation to show the effectiveness of FE. Benign noise shows smaller $-\log(p - value)$ values when compared to natural noise, indicating higher similarity in the feature space. Conversely, higher $-\log(p - value)$ values for malicious noise indicate significant differences compared to natural noise in the feature space.

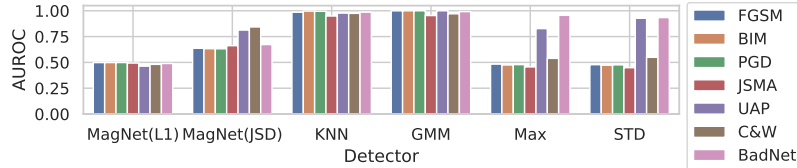
the target model under a black-box setting is not as effective. The table also highlights varying levels of transferability among different attacks. For instance, while most attacks almost entirely failed to transfer effectively, C&W and UAP attacks show partial transferability against the target model, with accuracies of 72.7% and 48.7%, respectively. Even though the attacks mostly fail to transfer to the target model, detecting such malicious attempts remains a formidable task. Hence, it would be intriguing if NOISEC can still detect such attempts, even in cases where the attacks completely fail to alter the model’s decision.

6.2 Detection Results

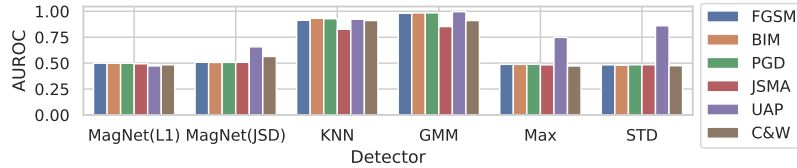
Effectiveness of Noise Representation This analysis evaluates the effectiveness of FE in capturing relevant features highly indicative of malicious attacks. For that, we compare the distribution of both the features of benign and malicious noises against the features of natural noises. First run the KS test between τ_{ben} and τ_{nat} and plot the $-\log(p - values)$ of each feature on Fig. 2. Here the smaller values for each feature indicate that τ_{ben} and τ_{nat} have almost similar distributions. Thus, the FE is effective in overlooking the random structures in the benign noise η_{ben} .

Contrarily, we run the similar KS test between τ_{mal} and τ_{nat} and plot their $-\log(p - values)$ on Fig. 2 values. Here, the higher $-\log(p - values)$ values prove that τ_{mal} and τ_{nat} have totally different distributions in most of the features. Such a finding reinforces our proposal to employ the target classifier itself as FE, with the objective of achieving effective AD through effective noise representation. This result further aligns with the conclusions drawn in [17], indicating that adversarial attacks stem from non-robust features, which appear random to human observers but are the target classifier can effectively detect them. Fig. 7 illustrates an exemplar of feature extraction under a representative (UAP) attack.

Effectiveness of Anomaly Detection Model. First, we analyze the effectiveness of different AD along with the MagNet baselines with respect to the



(a) Detection against white-box attacks.



(b) Detection against black-box attacks.

Fig. 3: Performance of different AD along with the MagNet baselines against white-Box and black-Box attacks. Fig. 5 & 6 in Appendix shows the ROC curves.

AUROC scores. Fig. 3(a) shows KNN and GMM-based ADs prove highly effective in distinguishing between benign and malicious instances across all attack types. Conversely, statistical detectors such as Max and STD exhibit only partial defense, particularly against UAP and BadNet attacks. As the perturbations under UAP and BadNet attacks have higher distortion, they are comparatively easier to detect after feature representation, even using simple statistical detectors. On the other hand, the other five attacks create subtle differences in the noise representation and need powerful ADs, like KNN and GMM. We advocate for these two, especially GMM, as a potential anomaly detector for future NOISEC applications. Moreover, the figure further shows that MagNet(L1) fails to detect white-box attacks, and MagNet(JSD) demonstrates only moderate defense against UAP and C&W attacks. MagNet(L1) failed as all the benign and malicious perturbations have the L1 norm.

In contrast, Fig. 3(b) presents a similar evaluation of attacks generated using the surrogate model and applied (and detected) against the target model. It is intriguing to note that although the transfer attacks mostly fail against the black-box target classifier, adversarial features within the noises still enable the target FE, allowing the detection of most attacks by KNN and GMM-based AD. On the other hand, both MagNet-based detectors completely failed to detect any black-box attacks. Therefore, even if the attacks can not directly compromise the target model’s performance, they leave detectable traces within the input data, which NOISEC can leverage.

Impact of Detection Threshold and FPR. Table 2 and Table 3 show the Precision, Recall, and F1-score of different NOISEC and MagNet detectors against the white-box, and black-box attacks, respectively. The detection threshold is

Table 2: NoiSEC with FPR < 1% under White-box Attacks.

Detector	FGSM			BIM			PGD		
	Pre	Rec	F1	Pre	Rec	F1	Pre	Rec	F1
MagNet(L1)	49.8	0.8	1.6	49.8	0.8	1.6	49.9	1.2	2.4
MagNet(JSD)	63.6	0.8	1.6	63.3	1.2	2.4	63.2	0.4	0.8
NoiSEC (KNN)	98.6	81.2	89.2	99.7	95.2	97.1	99.5	92.8	96.1
NoiSEC (GMM)	99.9	96.8	98.4	100.0	99.2	99.2	100.0	99.2	99.2

Continued

Detector	JSMA			C&W			UAP			BadNet		
	Pre	Rec	F1	Pre	Rec	F1	Pre	Rec	F1	Pre	Rec	F1
MagNet(L1)	49.4	0.8	1.6	48.1	0.4	0.8	46.4	0.4	0.8	48.9	1.2	2.4
MagNet(JSD)	66.2	0.4	0.8	84.3	22.8	36.9	81.3	22.0	35.8	67.3	32.4	48.8
NoiSEC (KNN)	94.9	74.8	0.8	97.5	43.2	60.0	97.7	76.8	86.7	98.7	72.4	83.6
NoiSEC (GMM)	95.4	80.4	87.7	97.1	59.2	74.0	100.0	100.0	99.8	99.2	89.6	94.1

Table 3: NoiSEC with FPR < 1% under Black-box Attacks.

Detector	FGSM			BIM			PGD		
	Pre	Rec	F1	Pre	Rec	F1	Pre	Rec	F1
MagNet(L1)	49.9	0.8	1.6	49.9	1.2	2.4	49.9	0.8	1.6
MagNet(JSD)	50.8	0.4	0.8	50.6	0.4	0.8	50.7	0.4	0.8
NoiSEC (KNN)	91.3	60.0	74.6	93.2	64.4	78.0	92.8	56.4	71.8
NoiSEC (GMM)	98.0	76.4	86.2	98.4	86.8	92.5	98.5	77.2	86.7

Continued

Detector	JSMA			C&W			UAP		
	Pre	Rec	F1	Pre	Rec	F1	Pre	Rec	F1
MagNet(L1)	49.3	0.8	1.6	48.4	0.8	1.6	47.3	0.8	1.6
MagNet(JSD)	50.8	0.8	1.6	56.4	0.8	1.6	65.7	0.0	0.0
NoiSEC (KNN)	82.7	31.6	47.7	91.1	18.8	31.4	92.3	51.2	67.4
NoiSEC (GMM)	85.2	31.2	47.3	91.1	12.8	22.5	99.6	86.4	92.3

carefully set to maintain an FPR rate within 1%. Notably, the NoiSEC equipped with a GMM-based detector exhibits superior performance, consistently maintaining high Precision, Recall, and F1-score across various attacks, particularly in the white-box scenario. However, under black-box attacks, while NoiSEC (GMM) maintains generally high detection rates for most attacks, it experiences reduced recalls for JSMA and C&W attacks, falling to 31.2% and 12.8%, respectively. This performance degradation can be attributed to the stringent maximum FPR criterion of 1%.

7 Conclusion

ML systems have become increasingly vulnerable to adversarial and backdoor attacks, which necessitates robust security measures. In this paper, we introduce NoiSEC, a detection method that only relies on noise to defend against such threats. NoiSEC is a reconstruction-based detector that isolates noise from test inputs, extracts malicious features, and utilizes them to identify malicious inputs. Experimental evaluations on the CIFAR10 dataset showcase the effectiveness of NoiSEC, achieving AUROC scores of over 0.954 and 0.852 against white-box and black-box adversarial attacks, respectively, and reaching 0.992 accuracy against backdoor attacks. Comparative study against MagNet-based approaches underscore NoiSEC’s superior performance across diverse attack scenarios.

References

1. Alex, K.: Learning multiple layers of features from tiny images. <https://www.cs.toronto.edu/kriz/learning-features-2009-TR.pdf> (2009)
2. Bai, T., Luo, J., Zhao, J., Wen, B., Wang, Q.: Recent advances in adversarial training for adversarial robustness. arXiv preprint arXiv:2102.01356 (2021)
3. Carlini, N., Wagner, D.: Towards evaluating the robustness of neural networks. In: 2017 IEEE Symposium on Security and Privacy (SP). pp. 39–57. Ieee (2017)
4. Demontis, A., Melis, M., Pintor, M., Jagielski, M., Biggio, B., Oprea, A., Nita-Rotaru, C., Roli, F.: Why do adversarial attacks transfer? explaining transferability of evasion and poisoning attacks. In: 28th USENIX security symposium (USENIX security 19). pp. 321–338 (2019)
5. Dempster, A.P., Laird, N.M., Rubin, D.B.: Maximum likelihood from incomplete data via the em algorithm. *Journal of the royal statistical society: series B (methodological)* **39**(1), 1–22 (1977)
6. Dong, S., Wang, P., Abbas, K.: A survey on deep learning and its applications. *Computer Science Review* **40**, 100379 (2021)
7. Feinman, R., Curtin, R.R., Shintre, S., Gardner, A.B.: Detecting adversarial samples from artifacts. arXiv preprint arXiv:1703.00410 (2017)
8. Fidel, G., Bitton, R., Shabtai, A.: When explainability meets adversarial learning: Detecting adversarial examples using shap signatures. In: 2020 international joint conference on neural networks (IJCNN). pp. 1–8. IEEE (2020)
9. Fix, E.: Discriminatory analysis: nonparametric discrimination, consistency properties, vol. 1. USAF school of Aviation Medicine (1985)
10. Goodfellow, I.J., Shlens, J., Szegedy, C.: Explaining and harnessing adversarial examples. arXiv preprint arXiv:1412.6572 (2014)
11. Grosse, K., Manoharan, P., Papernot, N., Backes, M., McDaniel, P.: On the (statistical) detection of adversarial examples. arXiv preprint arXiv:1702.06280 (2017)
12. Gu, T., Liu, K., Dolan-Gavitt, B., Garg, S.: Badnets: Evaluating backdoor- ing attacks on deep neural networks. *IEEE Access* **7**, 47230–47244 (2019). <https://doi.org/10.1109/ACCESS.2019.2909068>
13. Guo, C., Rana, M., Cisse, M., Van Der Maaten, L.: Countering adversarial images using input transformations. arXiv preprint arXiv:1711.00117 (2017)
14. Han, S., Lin, C., Shen, C., Wang, Q., Guan, X.: Interpreting adversarial examples in deep learning: A review. *ACM Computing Surveys* **55**(14s), 1–38 (2023)
15. Hanley, J.A., McNeil, B.J.: The meaning and use of the area under a receiver operating characteristic (roc) curve. *Radiology* **143**(1), 29–36 (1982)
16. He, K., Zhang, X., Ren, S., Sun, J.: Deep residual learning for image recognition. In: Proceedings of the IEEE conference on computer vision and pattern recognition. pp. 770–778 (2016)
17. Ilyas, A., Santurkar, S., Tsipras, D., Engstrom, L., Tran, B., Madry, A.: Adversarial examples are not bugs, they are features. *Advances in neural information processing systems* **32** (2019)
18. Kim, H.: Torchattacks: A pytorch repository for adversarial attacks. arXiv preprint arXiv:2010.01950 (2020)
19. Kurakin, A., Goodfellow, I.J., Bengio, S.: Adversarial examples in the physical world. In: Artificial intelligence safety and security, pp. 99–112. Chapman and Hall/CRC (2018)
20. Li, L., Xie, T., Li, B.: Sok: Certified robustness for deep neural networks. In: 2023 IEEE symposium on security and privacy (SP). pp. 1289–1310. IEEE (2023)

21. Li, Y., Jiang, Y., Li, Z., Xia, S.T.: Backdoor learning: A survey. *IEEE Transactions on Neural Networks and Learning Systems* (2022)
22. Liu, Y., Xie, Y., Srivastava, A.: Neural trojans. In: 2017 IEEE International Conference on Computer Design (ICCD). pp. 45–48. IEEE (2017)
23. Madry, A., Makelov, A., Schmidt, L., Tsipras, D., Vladu, A.: Towards deep learning models resistant to adversarial attacks. arXiv preprint arXiv:1706.06083 (2017)
24. Meng, D., Chen, H.: Magnet: a two-pronged defense against adversarial examples. In: Proceedings of the 2017 ACM SIGSAC conference on computer and communications security. pp. 135–147 (2017)
25. Mengara, O., Avila, A., Falk, T.H.: Backdoor attacks to deep neural networks: A survey of the literature, challenges, and future research directions. *IEEE Access* (2024)
26. Moosavi-Dezfooli, S.M., Fawzi, A., Fawzi, O., Frossard, P.: Universal adversarial perturbations. In: Proceedings of the IEEE conference on computer vision and pattern recognition. pp. 1765–1773 (2017)
27. Nicolae, M.I., Sinn, M., Tran, M.N., Buesser, B., Rawat, A., Wistuba, M., Zantedeschi, V., Baracaldo, N., Chen, B., Ludwig, H., Molloy, I., Edwards, B.: Adversarial robustness toolbox v1.2.0. CoRR **1807.01069** (2018), <https://arxiv.org/pdf/1807.01069>
28. Papernot, N., McDaniel, P., Goodfellow, I., Jha, S., Celik, Z.B., Swami, A.: Practical black-box attacks against machine learning. In: Proceedings of the 2017 ACM on Asia conference on computer and communications security. pp. 506–519 (2017)
29. Papernot, N., McDaniel, P., Jha, S., Fredrikson, M., Celik, Z.B., Swami, A.: The limitations of deep learning in adversarial settings. In: 2016 IEEE European symposium on security and privacy (EuroS&P). pp. 372–387. IEEE (2016)
30. Paszke, A., Gross, S., Massa, F., Lerer, A., Bradbury, J., Chanan, G., Killeen, T., Lin, Z., Gimelshein, N., Antiga, L., et al.: Pytorch: An imperative style, high-performance deep learning library. *Advances in neural information processing systems* **32** (2019)
31. Press, W.H.: Numerical recipes 3rd edition: The art of scientific computing. Cambridge university press (2007)
32. Szegedy, C., Zaremba, W., Sutskever, I., Bruna, J., Erhan, D., Goodfellow, I., Fergus, R.: Intriguing properties of neural networks. arXiv preprint arXiv:1312.6199 (2013)
33. Vassilev, A., Oprea, A., Fordyce, A., Anderson, H.: Adversarial machine learning: A taxonomy and terminology of attacks and mitigations. Tech. rep., National Institute of Standards and Technology (2024)
34. Wang, N., Chen, Y., Xiao, Y., Hu, Y., Lou, W., Hou, Y.T.: Manda: On adversarial example detection for network intrusion detection system. *IEEE Transactions on Dependable and Secure Computing* **20**(2), 1139–1153 (2022)
35. Weng, C.H., Lee, Y.T., Wu, S.H.B.: On the trade-off between adversarial and backdoor robustness. *Advances in Neural Information Processing Systems* **33**, 11973–11983 (2020)
36. Zhao, Y., Nasrullah, Z., Li, Z.: Pyod: A python toolbox for scalable outlier detection. *Journal of machine learning research* **20**(96), 1–7 (2019)

A Appendix

Table 4: Autoencoder Architecture for CIFAR-10

Encoder			Decoder		
Layer	Kernel	Output	Layer	Kernel	Output
Conv2D	3x3/32	32x32x32	Linear	-	8192
Conv2D	3x3/32	32x32x32	Reshape	-	128x8x8
Conv2D	3x3/64	64x16x16	ConvTrans2D	3x3/128	128x8x8
Conv2D	3x3/64	64x16x16	ConvTrans2D	3x3/64	64x16x16
Conv2D	3x3/128	128x8x8	ConvTrans2D	3x3/64	64x16x16
Conv2D	3x3/128	128x8x8	ConvTrans2D	3x3/32	32x32x32
Flatten	-	8192	ConvTrans2D	3x3/32	32x32x32
Linear	-	1024	ConvTrans2D	3x3/3	3x32x32

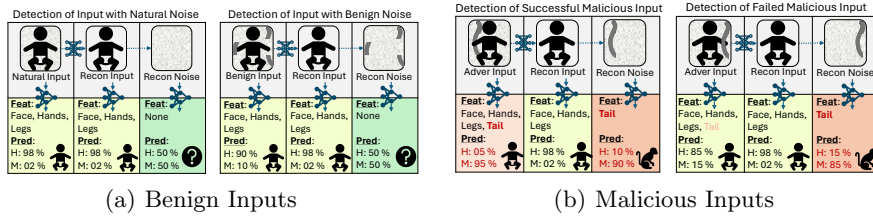


Fig. 4: Examples illustrating the fundamental intuition behind NoISEC’s detection technique using a binary detector (human vs. money). In benign inputs, the reconstruction noise lacks prominent features. However, in both successful and unsuccessful malicious inputs, the reconstruction noise reveals a detectable perturbation resembling a tail, enhancing the effectiveness of detection.

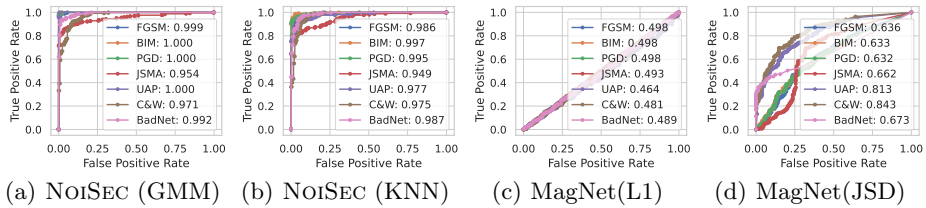


Fig. 5: ROC curve with AUROC score of different AD against white-box attacks.

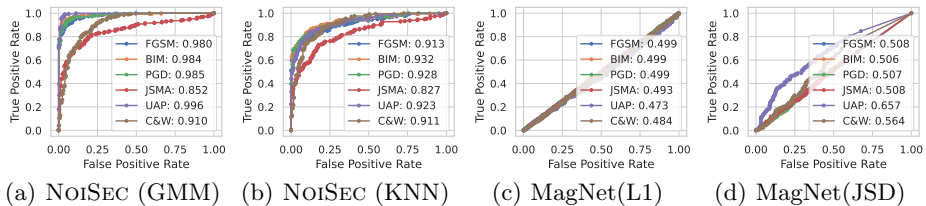


Fig. 6: ROC curve with AUROC score of different AD against black-box attacks.

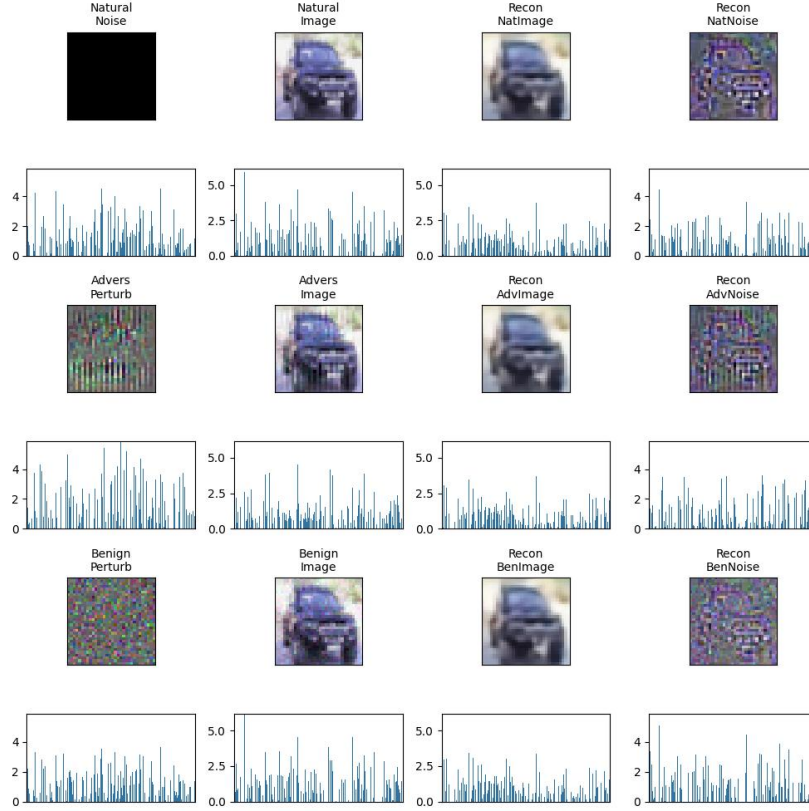


Fig. 7: Analysis of NoiSEC on three types of inputs: natural, adversarial, and benign input. The top row illustrates the reconstruction process of a natural image with no added noise. The reconstructed natural image (Recon NetImage) shows the key component of the car, while the reconstructed natural noise (Recon NatNoise) displays the inherent noise in the natural image. The barplot below each image represents the features extracted by FE. Similarly, the second and third image rows depict the reconstruction process of an adversarial example (UAP attack) and benign input (random noise), respectively. Noticeably, the reconstructed adversarial noise (Recon AdvNoise) predominantly consists of the adversarial perturbation (Advers Perturb) added during the generation of the adversarial image, whereas the reconstructed benign noise closely resembles random noise. A detailed visual examination reveals a degree of similarity between the extracted features from the reconstructed natural and benign noises, whereas the features of reconstructed adversarial noise exhibit subtle differences.